

STRENGTH AND BEHAVIOR OF COMPOSITE STEEL TUBE CONCRETE BEAM

Wissam D. Salman

Lecturer, College of Engineering, University of Diyala

dr_wissam80@yahoo.com

(Received: 21/9/2014; Accepted: 9/11/2014)

ABSTRACT: - This paper deals with an experimental and analytical study to investigate the structural behavior of simply supported composite steel-concrete tube beams with external load, in which a concrete is connected together with steel circular tube by means of headed stud shear connectors. This type of structure not only inherits the characteristics of traditional concrete tube beams but also possesses its own unique attributes, such as advantageous mechanical performances, facilitating construction process, and low maintenance cost etc. Seven composite steel-concrete tube beams were tested to their ultimate strength. The effect of thickness and diameter of steel tube on structural performance of composite beams were investigated. Experimental results proved that, due to increase tube thickness from (2mm to 6mm), the strength increased by (63.5%) and the ultimate deflection increased by (75%). While the strength increased by (190.3%) and the ultimate deflection decreased by (47%) when the tube diameter increased from (75mm to 200mm). Based on the experimental results, a theoretical model for predicating the flexural resistance of composite steel- concrete tube beam is proposed. ANSYS computer program (version 13.0) has been used. The calculated flexural resistance based on proposed model has a high level of accuracy when compared with test results.

Keywords: composite beams; ANSYS; steel–concrete tube beam; non-linear analysis.

1. INTRODUCTION:

The term “composite construction” is normally understood within the context of buildings and other civil engineering structures to imply the use of steel and concrete formed together into a component in such a way that the resulting arrangement functions as a single item. The aim is to achieve a higher level of performance than would have been the case had the two materials functioned separately. Thus the design must recognize inherent differences in properties and ensure that the structural system properly accommodates. Composite

construction refers to any members composed of more than one material. The parts of these composite members are rigidly connected such that no relative movement can occur.

Composite steel-concrete beams have been widely used in civil engineering, because of their economic benefits and good structural behavior. Numerous research papers were published which related to composite steel and concrete beams, such as Lili Wu ⁽¹⁾ presented a new type of steel-concrete composite beam where the beam is featured with a channel shaped section, the U-section steel beam is prefabricated with steel plates and the interior side of the channel is cast with concrete. Preliminary research was conducted on its bending capacity, stiffness, stress distribution, crack diagram etc. Experimental results revealed that the steel plates and the concrete slab integrated through shear stud connectors can work well together and the channel beam model presented a bending failure mode.

Huiyong Ban ⁽²⁾ published a research of HS steel-concrete composite beams, forty beams with various steel grades and degrees of shear connection are modeled. New design approaches are proposed in order to estimate the bending behavior of simply supported composite beams with HS steel, providing more reliable and economical design solutions for such members.

Tan ⁽³⁾ provides results from several tests to support the view that in the presence of flexure in curved composite beams, there will be an increase in the torsional moment capacity, but the flexural moment capacity does not greatly increase in the presence of torsion. Ranzi ⁽⁴⁾ investigated the structural behavior of simply supported composite beams with large rectangular web openings; two-dimensional finite element models employing plane stress elements are established. Other research papers were published which related to composite steel and concrete box girders, such as references (5 to 7) etc. Many significant research results have been achieved in understanding the structural behavior of composite steel-concrete beams. In this paper, a new formulation for studying simple composite beams with circular tube is proposed.

2. EXPERIMENTAL PROGRAM

2.1 DETAILS OF TEST SPECIMENS

Seven composite steel-concrete tube beams were designed and constructed in this study, four of them with different thickness of steel tube (2mm, 3mm, 4mm, and 6mm) with the same diameter (100mm) were loaded under positive bending moments, designated (CB1 ,CB2, CB3 and CB4) respectively. And the other three beams with constant thickness of (4mm) and different diameter of steel tube (75mm, 100mm, and 200mm) designated (CB5, CB6, and CB7) respectively.

The typical entire shape of any of those seven test specimens is shown in Figure (1). The typical specimen's length of all beams is (2000mm) and consisted of a reinforced concrete slab at the top and a circular steel tube at the bottom connected together by means of headed stud shear connectors welded to the steel tube. The concrete slab had a depth of (100mm) and a width of (400mm) and reinforced with one layer of rebar in two directions ($\text{Ø}5\text{mm} @ 50\text{mm}$ in each direction) as well as the reinforcing bars provided at support as shown in Figure (2).

In each specimen two supports are provided in the end of the test specimen with (300mm) width and (250mm) length in order to easily put the specimen in the flexural test instrument. 24 shear studs with (8.8mm) diameter and a height of (60mm) were welded on the top of steel tube to ensure anchorage in the concrete except CB3 with (60) shear stud. The center to center distance of the supporting girders was (1800mm). The measured mean compressive strength of the concrete using cylinders (150mm \times 300mm) is (44MPa) and the average tensile strength is (3.4MPa). The steel used for the circular -section beam has a mean tensile yield strength f_y of (375MPa). The geometric properties of all the specimens are shown in Table (1).

2.2 INSTRUMENTATION

The specimens were instrumented for the purpose of measuring deflections, concrete strain, applied load, and slips between the steel tube and the concrete slab. All beam specimens were tested by using the universal testing machine (MFL system) under monotonic loads to ultimate states. The test beams were simply supported over an effective span of (1800mm) and loaded with two-point loads. The distance between the two point loads was kept constant at (600mm). The applied loads were distributed across the entire width of the upper concrete face. Relative thick rubber strips were inserted between the concrete and line loads, as well as between support of machine and lower support face of specimen. The loads were applied in successive increments up to failure. At the end of each load increment, observations and measurements were recorded for the mid-span deflection, end slip, strain gage readings and crack development.

The vertical deflections have been measured at three points as central deflection and at third span using mechanical dial gauge of (0.01mm) accuracy with (50mm) total stroke, the dial gauges has been attached to the soffit of the tested beams, as shown in Figure (3). Two linear variable displacement transducers (LVDTs) were located at each end support of the composite steel concrete beams to measure the maximum interface slip between the concrete slab and the steel beam during testing. Concrete compressive strains have been measured using Demec points, aluminum discs with (8mm) diameter and (1mm) diameter hole at the center. Demec discs are mounted in three locations on the top face of the beam. A digital

extensometer with (0.001mm) accuracy, as shown in Figure (4), was used to measure relative movement of the Demec points, from which the longitudinal strain is calculated for each load increment. The digital extensometer is capable of measuring displacement changes between two Demec strain discs fixed at (100mm) gauge length. All beams were tested at ages of (30-38) days. The beam specimens were placed on the testing machine and adjusted so that the centerline, supports, point loads and dial gauges were fixed in their correct or proper locations.

To measure crack widths, an optical micrometer with an accuracy of (0.02mm), as shown in Figure (5) was used for all beams specimens. The beam surfaces were painted with white color to make it easy to see the crack and measure its width.

2.3 MATERIALS

Each test specimen was made of different materials and components i.e. steel tube, concrete, shear connectors and reinforcing bars, which were assembled together to constitute a composite steel-concrete tube beam. These materials have possibly important effects on the structural response of the test specimens and must be individually evaluated.

2.3.1 STEEL

In the fabrication process of the test specimens, steel material was used in three situations, circular tubes, reinforcing bars of concrete slab and headed stud shear connectors.

2.3.1.1 STEEL CIRCULAR TUBES

In the four first specimens (CB1, CB2, CB3 and CB4) of (2mm, 3mm, 4mm and 6mm) thickness, respectively was used steel circular hollow tube with (2000mm) length and the diameter is (100mm). In other specimen used steel circular hollow tube with (2000mm) length and (4mm thickness). The diameter of steel tube (CB5, CB6 and CB7) were used (75mm, 100mm and 200mm) respectively. The typical shape of the three circular tubes is shown in Figure (6). The shear connectors are welded to steel tube in order to provide full bond between steel tube and concrete to prevent slip between them.

2.3.1.2 REINFORCING STEEL BARS

One layer of (5mm) diameter deformed bars was used in the longitudinal as well as the transverse direction of the reinforced concrete slab, the reinforcing bars provided at support as shown in Figure (2).

2.3.1.3 SHEAR CONNECTORES

To resist the longitudinal shear at the interface between steel girder and concrete slab, and to prevent the vertical separation between them, headed stud shear connectors of diameter (8.8mm) and overall length (63mm) with a head of diameter (16mm) and height

(6mm) were used in each test specimen. The bolt consisted of hexagonal head. These studs were welded on the steel circular tube as shown in Figure (7).

3.3.2 CONCRETE

The materials used in producing concrete are locally available materials, which include cement, crushed coarse gravel, natural silica sand and water. Ordinary Portland cement (karasta cement) as used throughout the investigation. The whole required quantity was brought to the laboratory and stored in a dry place. Natural silica sand was used as fine aggregate with maximum size of (4.75mm) while natural gravel was used as coarse aggregate with maximum size of (10mm). The natural gravel was washed and left in air, and then stored in a saturated dry surface condition before use. The ordinary potable water was used in making concrete and curing.

The same concrete mix was used through the whole investigation. The mix properties of the ingredients by weights were [1 cement: 1.6 sand: 1.9 gravel], and water cement (w/c) ratio was 50%, to give slump of about (120mm).

Mixing was manually carried out in the Structures tests Laboratory of the College of Engineering at the University of Diyala. The surfaces of the pan and the mixing tools were cleaned and moistened before use. The dry ingredients were added in the following order, about one half of the coarse aggregate, all the fine aggregate, all the cement, and finally the remaining part of coarse aggregate. Then water was added and mixing was started. The period of mixing ranged from five to seven minutes. The specimen is vibrated by a rode vibrator with a compaction time (2minutes) for each layer. The cubes and prisms molds were filled with concrete in two equal layers, while the cylinder specimens were cast in equal three layers. After the top layer had been compacted, it was leveled by using a steel trowel.

3- EXPERIMENTAL RESULTS AND DISCUSSION

3.1 ULTIMATE LOAD (P_U)

The load on specimens is applied monotonically in increments. These increments are reduced in magnitude as the load reaches the ultimate load. The maximum load recorded by the testing machine is considered as the ultimate load and is given in Table (2). Test results show that, due to increase the tube thickness from (2mm to 6mm) the strength increased by (63.5%) and the strength increased by (190.3%) when the tube diameter increased from (75mm to 200mm) this is due to increase in moment of inertia of section caused increasing in ultimate strength.

3.2 DEFLECTION

Figure (8) shows the load-deflection diagram for all the seven composite steel-concrete tube beams measured at the mid-span of the beams. These Figures show that the load-deflections curves are very close results at the early stages of load history for all analysis conducted, having initially linear relation with a sudden loss of stiffness when cracking of concrete begins.

Form Figure (8) all curves at the beginning were identical and the tested beams exhibited linear behavior and the initial change of slope of the load-deflection curves were (40kN, 80kN, 80kN, and 140kN) for (CB1, CB2, CB3, and CB4) respectively and (60kN, 85kN, and 170kN) for (CB5, CB6, and CB7) respectively. Test results show that the large deflection is at reference beam (CB5) which has (75mm) diameter steel tube. As shown in Table (2) the tested beam (CB6) which have (100mm) diameter steel tube, the decreases in deflection was (20%) from reference beam (CB5), and the tested beam (CB7) which have (200mm) diameter steel tube, the decreases in deflection was (46.7%) from the reference beam (CB5).

3.3 INTERFACE SLIP (SHEAR SLIP)

Using linear variable differential transducers (LVDTs), the interface slip between the concrete slab and the steel tube was measured and summarized in Table (3). These measurements were taken at the support ends of the composite steel-concrete tube beam, where the interface slip was the highest. Relative interface slip was recorded as well when the maximum applied load was reached. The value of interface slip at the first specimen was plotted against the applied load and shown in Figure (9). As expected, higher interface slip is required for the composite steel-concrete tube beam when larger thickness was used. For example, CB1 reached a relative interface slip of (2.0mm) compared with that of (2.65) mm for CB4. The ultimate slipping of ultimate load was increased from (2 to 2.65mm) with increasing thickness diameter of steel tube from (2 to 6mm) for (CB1 and CB4) respectively, but CB3 decrease slipping was (1.25mm) because the effect of length support and increasing the number of shear connectors. Results show that no sufficient data about the slip in CB2 because problem in support due to the shear that happened only in CB2. The development of interface slip and horizontal cracks due to shear slip is shown in Figure (10).

3-4 CONCRETE STRAIN

The strains in the concrete at the mid-span section of the test specimens were measured by using 100mm demec gauge over the top fiber of the beam. Figure (11) shows the load versus extreme compression fiber strain response of the concrete slab observed from experimental test for all beams. From these Figures, it can be seen that the strain distribution

remained approximately linear at low loads and became nonlinear at higher loads due to cracking. Average strain for CB2, CB3 and CB4 decreased with increasing load comparing with CB1 shown that effect thickness of steel tube on strain. For all tests specimen were strain more than (0.002) at ultimate load except specimen CB2 was (0.0013). The demec disc for CB7 is separated during the test for this reason no data about the strain of CB7. The strain in CB5 and CB6 with (33.33%) different in steel tube diameter, at load (115kN) the increasing in steel tube lead to decreasing in strain about (77.3%).

3-5 CONCRETE CRACKS

During testing surface of concrete is carefully inspected for developing cracks, the cracks in CB1, CB2, CB3 and CB4 appeared at the bottom surface of concrete slab in the region of maximum positive bending moment. In CB3 cracks appeared in support and longitudinal cracks in concrete slab, and the number of cracks were equal in CB1 and CB2 about (10) but in CB3 was (9) and in CB4 was (8). In CB7 at first shear cracks appeared in support and longitudinal cracks formed in concrete slab due to the lateral tensile forces induced in the slab caused by the dowel action of individual shear connectors then cracks began to appear at max bending moment zone. The cracks in all CB5, CB6 and CB7 appeared at the extreme tension fibers (bottom surface of concrete slab) in the region of maximum positive bending moment. Figure (12) shows the tension cracks in test specimens while Figure (13) shows cracks in support in CB7.

4- NUMERICAL SIMULATION OF EXPERIMENT

The FE analysis of the test beams under pure bending was carried out by using nonlinear FE software ANSYS 13. The primary aim of the numerical simulation was to validate the employed FE modeling by comparing with the experimental results.

4.1 FINITE ELEMENT MODELING

ANSYS 13 program was used to analyze the three dimensional model. The concrete was modeled by using the 8-noded isoperimetric brick elements (SOLID 65). The element is defined by eight nodes having three degrees of freedom at each node, translation in the x, y, and z directions. The element is capable of modifying cracks in tension and in three orthogonal directions, crushing in compression, and plastic deformation.

The steel bars were modeled using axial members (LINK8). This element can be used to model trusses, sagging cables, links, springs, etc. The 3-D spar element is a uniaxial tension compression element with three degrees of freedom at each node: translations of the nodes in x, y, and z-directions. As in a pin-jointed structure, no bending of the element is considered. Plasticity, creep, swelling, stress stiffening, and large deflection capabilities are included. The steel tube beam was modeled using isoperimetric shell elements (SHELL43) with 4-nodes.

SHELL43 is well suited to model linear, warped, moderately-thick shell structures. The element has six degrees of freedom at each node: translations in the nodal x, y, and z directions and rotations about the nodal x, y, and z axes. The deformation shapes are linear in both in-plane directions. For the out-of-plane motion, it uses a mixed interpolation of torsorial components. The element has plasticity, creep, stress stiffening, large deflection, and large strain capabilities.

A (COMBIN39) nonlinear spring elements was used to represent the shear connectors with link 8. The element COMBIN 39 is a unidirectional element (or nonlinear spring) with nonlinear generalized force deflection capability that can be used in any analysis. The element has a large displacement capability for which there can be two or three degrees of freedom at each node. The element is defined by two nodes and a generalized force deflection curve.

For nonlinear solution, ANSYS "Newton-Raphson" approach to solve nonlinear problems. In this approach, the load is subdivided into a series of the load increments. The load increments can be applied over several load steps. A typical finite element mesh for the composite beam is shown in Figure (14).

4.2 RESULTS AND DISCUSSION

4.2.1 LOAD DEFLECTION CURVES

To compare the load-deflection curve of F.E. Model together with experimental test curves, it is necessary to measure the vertical displacement (deflection) at centerline of bottom face of the F.E. Model. The experimental and analytical load-deflection curves are shown in Figure (15) and Figure (16). Good agreement is obtained between the predicted finite element and the experimental load-deflection curves throughout the entire range of behavior of the tested beams. The midspan externally applied load is plotted against the midspan deflection.

4.2.2 ULTIMATE LOAD AT FAILURE REGION

In finite element analysis, "Ultimate load" which the beam can carry by finite element Model is defined as the final load for cumulative substeps to the last applied sub step before solution starts diverging due to numerous crack and large deflection after steel yielding. Comparison between this value $(P_u)_{FEM}$ and the ultimate load (collapse load) of experimental test beam $(P_u)_{EXP}$ is given in Table (4). In this table, good agreement can be noted between these values and it shows that, the percent discrepancy of finite element model.

4.2.3 LOAD-STRAIN CURVES

Figure (17) and Figure (18) show the load versus extreme compression fiber strain response of the concrete slab observed from experimental and analytical study (ANSYS

software) of all tested beams. It is shown that the analytical compressive strains and corresponding experimental strains are very close throughout the loading up to the yielding then the analytical strain become slightly lower than the experimental strain up to ultimate load.

4.2.4 LOAD-SLIP CURVES

Numerically, the relative movement (shear slip) between concrete and steel tube beam was measured from the difference between the nodal displacements, in x-direction (U_x), at concrete and steel tube beam. Figure (19) and Figure (20) show load-slip relationships for all tested beams. It is cleared a good agreement can be noted between experimental and finite element Model. Result show that no sufficient data about the slip in CB2 because problem in support due to the shear that happened only in CB2.

5- CONCLUSIONS

Based on the results obtained from this study, the followings can be concluded:

- 1- The general trend in ultimate load values (P_u) for each specimen, is to increase by increasing the thickness and diameter of steel tube, (50% to 200%) increasing in steel tube thickness lead to (30.4% to 63.5%) increasing in ultimate load, (33.3% to 166.7%) increasing in steel tube diameter lead to (32.7% to 190.3%) increasing in ultimate load.
- 2- The vertical ultimate deflection for each specimen increase by increasing the thickness of steel tube, (50% to 200%) increasing in steel tube thickness lead to (40.3% to 74.7%) increasing in vertical ultimate deflection. While vertical ultimate deflection decrease by increasing the diameter of steel tube, (33.3% to 166.7%) increasing in steel tube diameter lead to (20% to 46.7%) decreasing in vertical ultimate deflection.
- 3- The ultimate slip at the ultimate load, for each specimen, is to increasing by increasing the thickness of steel tube, (2-6) mm increasing the steel tube thickness lead to (2-2.65) mm increasing in the ultimate slip at the ultimate load.
- 4- The strain, for each specimen, is to increase by increasing the thickness of steel tube.
- 5- The ultimate slip at the ultimate load, for CB3 and CB6 is to decreasing by increasing the length of support, (250-500) mm increasing the length of support, (6.4-1.25) mm decreasing the ultimate slip at the ultimate load.
- 6- The finite element model used in the present work is able to simulate the behavior of composite steel-concrete tube beams in flexure. The analytical studied indicated that the load-deflection behavior and the ultimate loads are in good agreement with the published experimental results.

6- REFERENCES

- 1) Lili Wu, Jianguo Nie, Jianfeng Lu, Jiansheng Fan, and C.S. Caic, (2013), “A new Type of Steel-Concrete Composite Channel Girder and Its Preliminary Experimental Study” jcsr, Elsevier. June, Vol. 85, p163-177.
- 2) Huiyong Ban, Mark A. Bradford, (2013) “Flexural Behavior of Composite Beams with High Strength Steel”, Engineering Structures, Elsevier. Nov, Vol. 56, p1130-1141.
- 3) Tan E.L., Uy B., (2009) “Experimental Study on Curved Composite Beams Subjected to Combined Flexure and Torsion” jcsr, Elsevier, Vol. 65, p1855-1863.
- 4) Ranzi G, Zona A., (2007) “A Steel–Concrete Composite Beam Model with Partial Interaction Including the Shear Deformability of the Steel Component” Engineering Structures, Elsevier, Vol 29 pp 3026–3041.
- 5) Yasir I. Musa , Manuel A. Diaz, (2007) “Design Optimization of Composite Steel Box Girder in Flexure” Structural Design and Construction, ASCE, Aug, Vol. 12, No. 3, pp. 146-152.
- 6) Yasunori Arizumi; Sumio Hamada; and Takeshi Oshiro, (1988) “Behavior Study of Curved Composite Box Girders” Journal of Structural Engineering, ASCE, Nov, Vol. 114, pp. 2555-2573.
- 7) Wu, Y. Lai, Y. Zhang, X. Zhu, Y., (2004) “A Finite Beam Element for Analyzing Shear Lag and Shear Deformation Effects in Composite-Laminated Box Girders” Computers and Structures., Elsevier, Vol. 82 pp 763-771.

Table (1): Details of specimens.

Specimen	d_s (mm)	t_s (mm)	No. of shear connectors	Length of support (mm)
CB1	100	2	24	250
CB2	100	3	24	250
CB3	100	4	60	500
CB4	100	6	24	250
CB5	75	4	24	250
CB6	100	4	24	250
CB7	200	4	24	250

Where d_s and t_s are the diameter and thickness of steel tube respectively

Table (2): Ultimate load and maximum deflection for tested specimens.

Specimen	P_u (kN)	Δ_{max} (mm)	% of Increase in P_u	% of Increase in Δ_{max}
CB1*	115	26.05	----	----
CB2	150	36.54	30.4	40.3
CB3	166	37.80	44.3	45.1
CB4	188	45.50	63.5	74.7
CB5*	113	45.00	----	----
CB6	150	36.00	32.7	-20.0
CB7	328	24.00	190.3	-46.7

* Reference Beam

Table (3): Slip values for test specimens.

Specimens	Maximum interface slip (mm)
CB1	2.0
CB2	-
CB3	1.25
CB4	2.65
CB5	3
CB6	6.3
CB7	2.2

Table (4): Ultimate loads from experimental tests and finite element analysis.

Specimen	Ultimate Load (kN)		$\frac{(P_u)_{FEM}}{(P_u)_{EXP}}$	Difference Ratio
	$(P_u)_{FEM}$	$(P_u)_{EXP}$		
CB1	112	115	0.974	2.6%
CB2	144	150	0.960	4%
CB3	174	166	1.048	4.8%
CB4	179	188	0.952	4.8%
CB5	112	113	0.991	0.9%
CB6	148	150	0.987	1.3%
CB7	324	328	0.988	1.2%

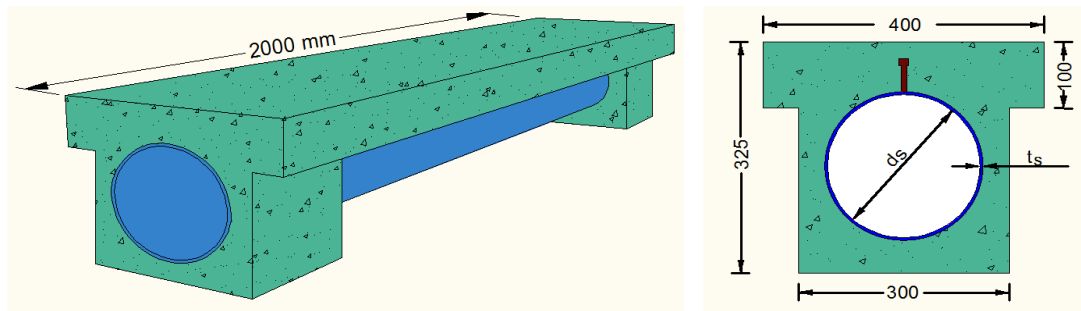


Figure (1): Typical shape and dimension of composite steel tube concrete beam specimen.



Figure (2): Reinforcement of composite steel tube concrete beam specimen.



Figure (3): Composite steel tube concrete beam specimen under test



Figure (4): Digital extensometer and demec discs.



Figure (5): Optical micro-meter.

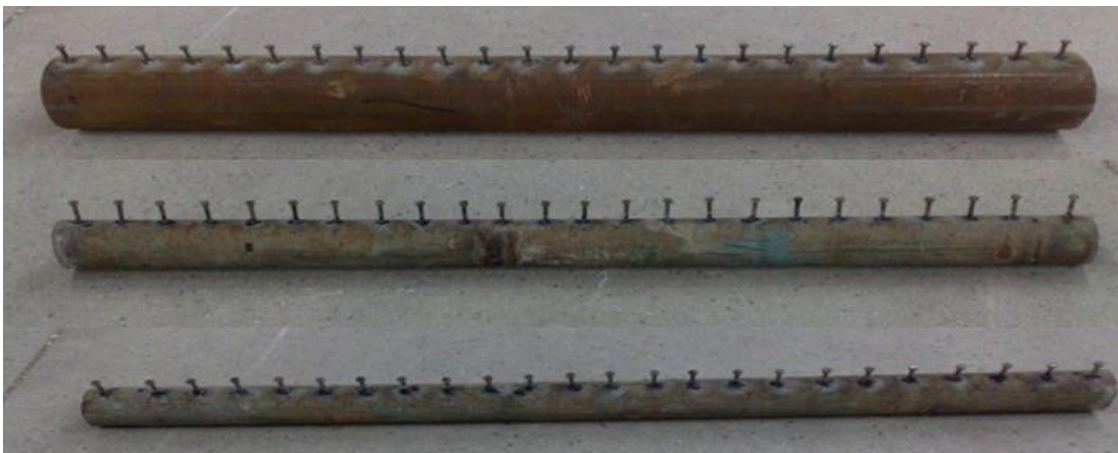


Figure (6): Circular steel tubes with different diameter.



Figure (7): Head stud shear connector.

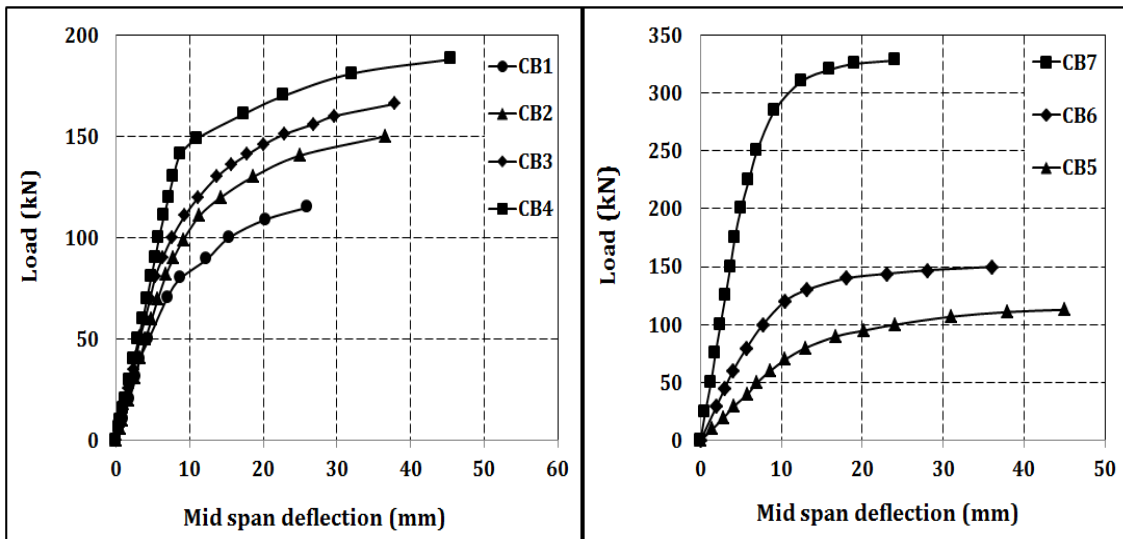


Figure (8): Load- deflection relationship for the tested specimens.

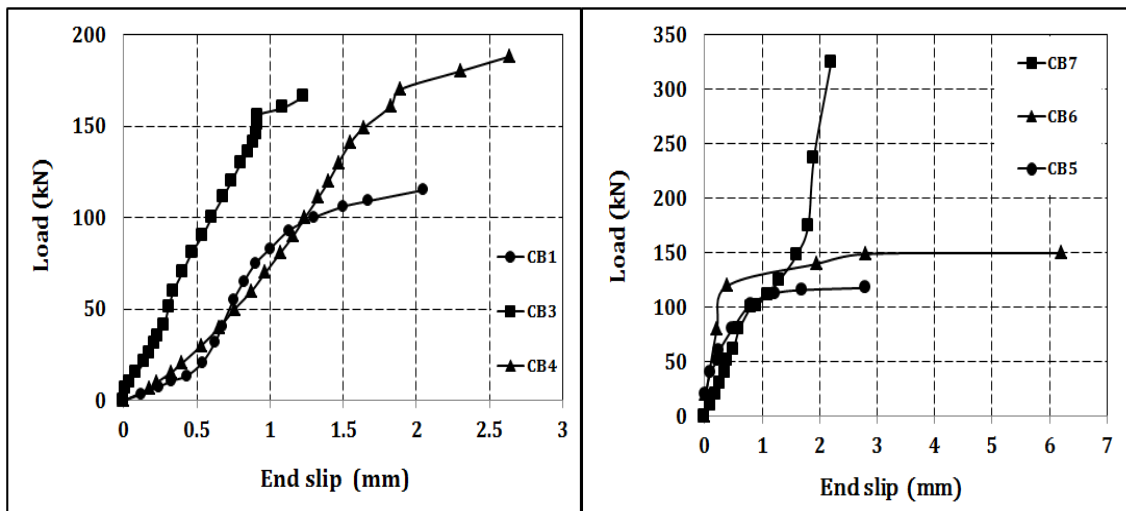


Figure (9): Load-slip relationship for test specimens.

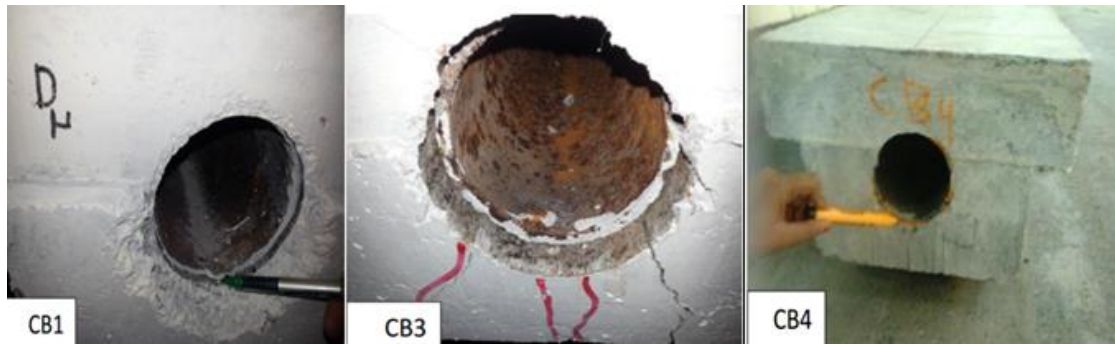


Figure (10): Slip between interfaces

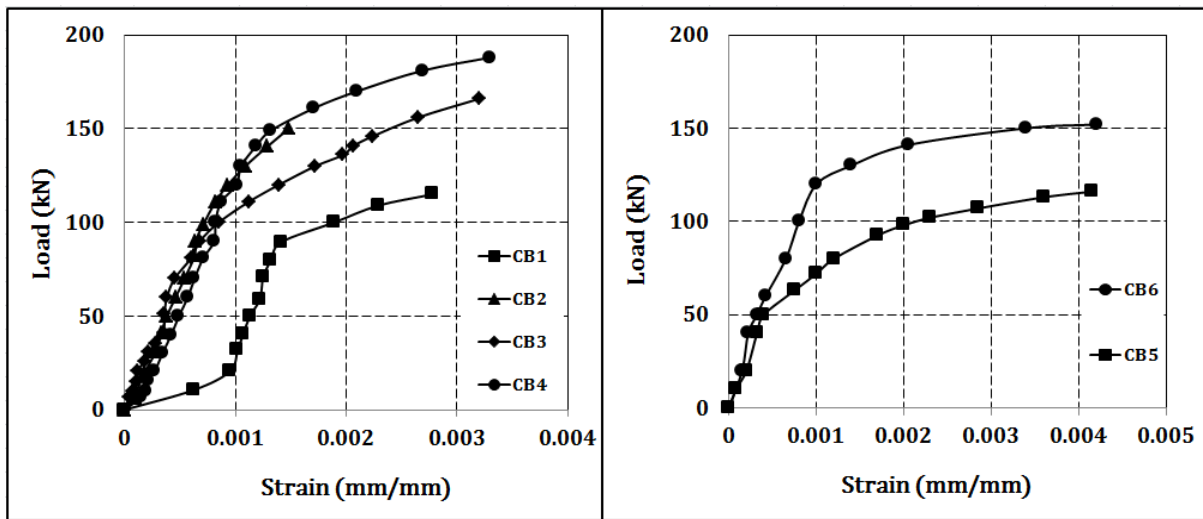


Figure (11): Load-strain relationship for test specimens.

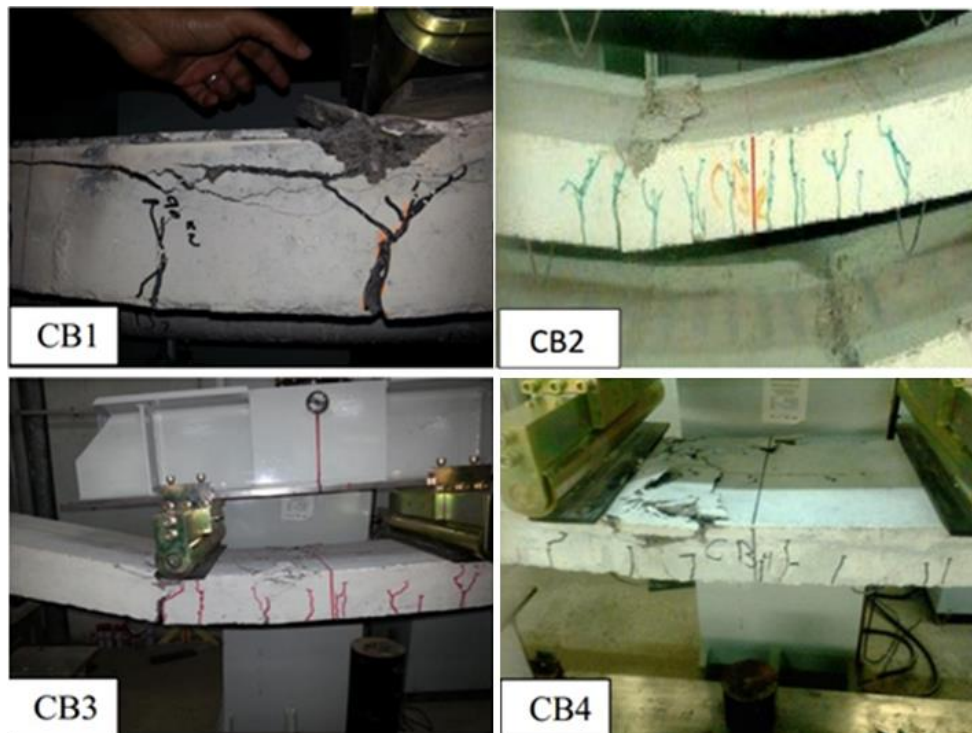


Figure (12): Tension cracks in test specimens.



Figure (13): Shear cracks at support in beam CB7.

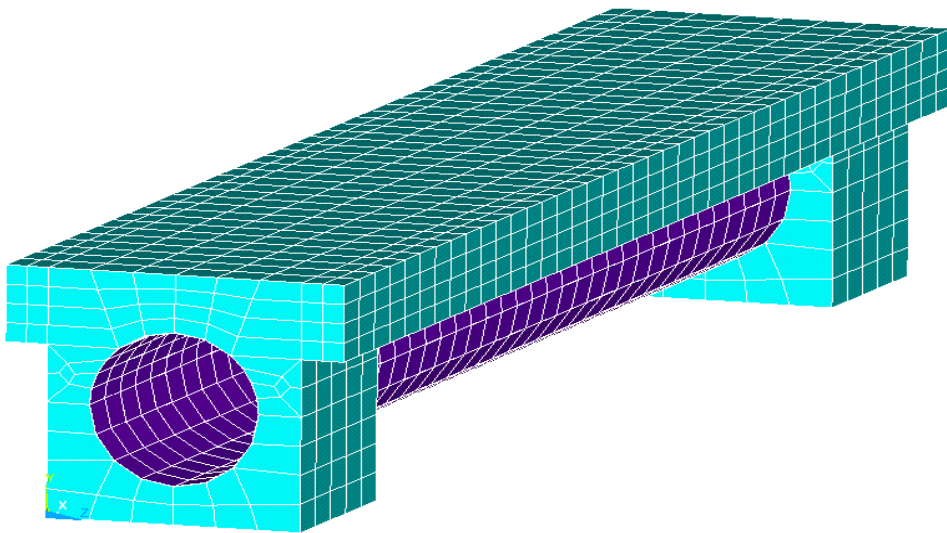


Figure (14): Finite element mesh of composite steel tube concrete beam specimen.

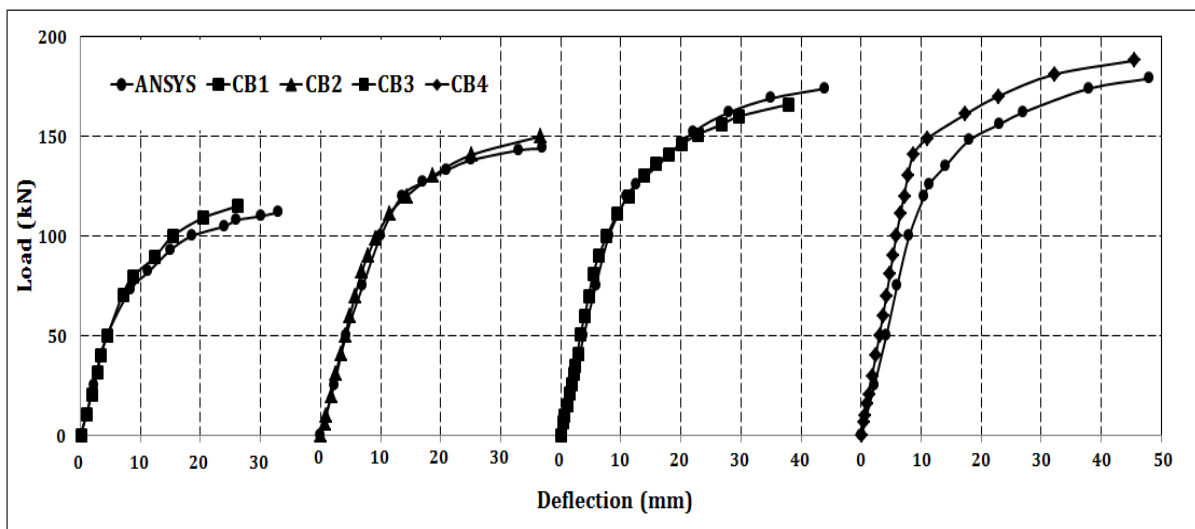


Figure (15): Load-deflection curves from experimental test and finite element analysis (part 1).

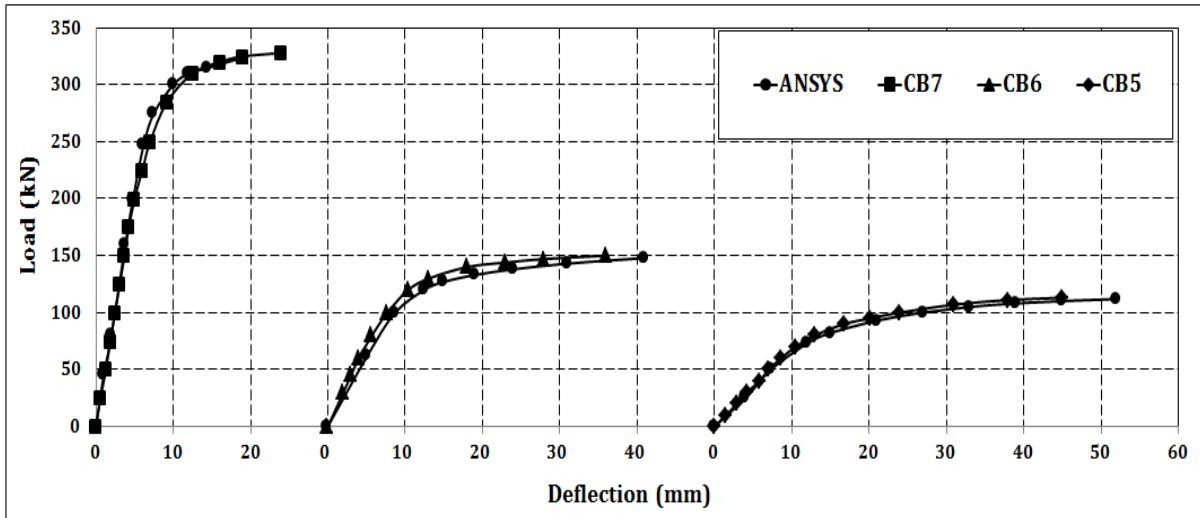


Figure (16): Load-deflection curves from experimental test and finite element analysis.

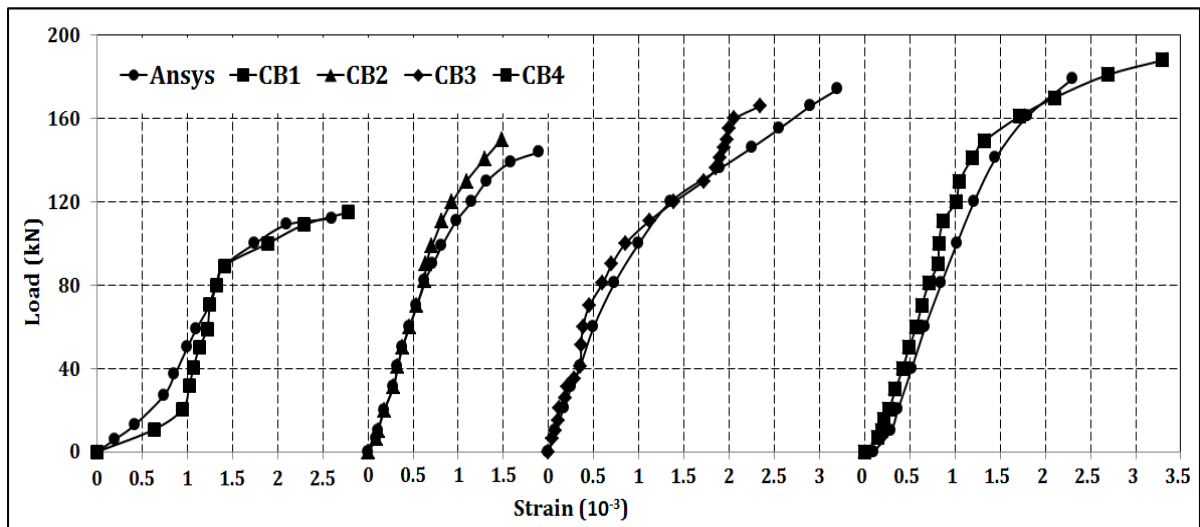


Figure (17): Mid-span strain curves from experimental test and finite element analysis (part 1).

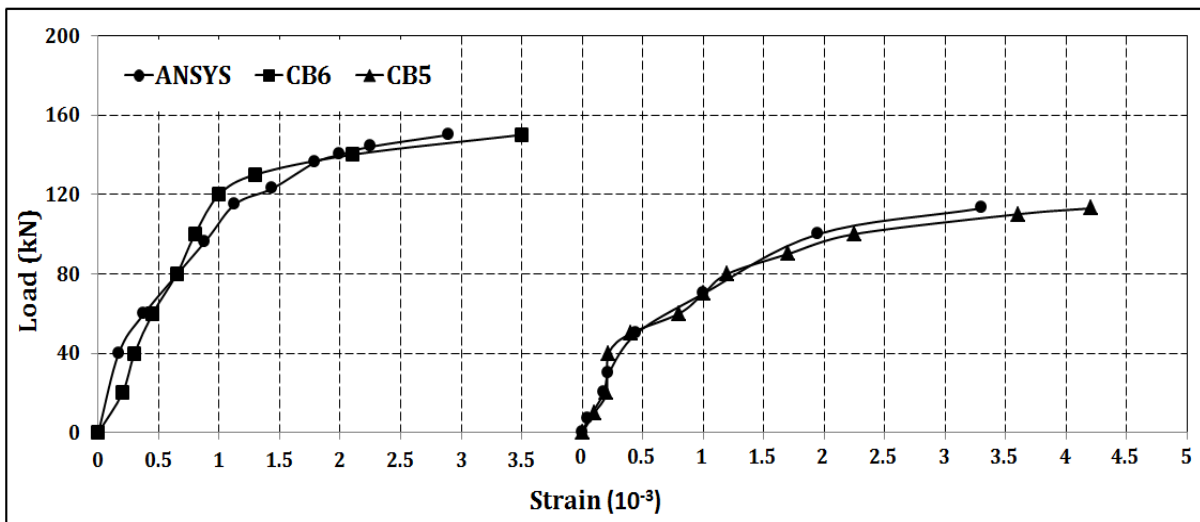


Figure (18) Mid-span strain curves from experimental test and finite element analysis (part 2).

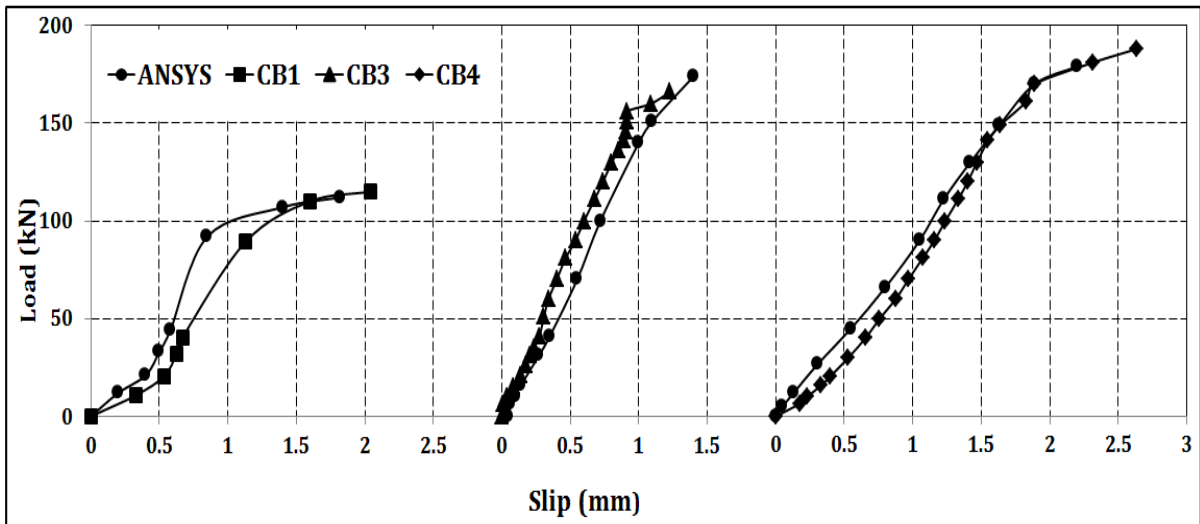


Figure (19): Slip-load curves from experimental test and finite element analysis (part 1).

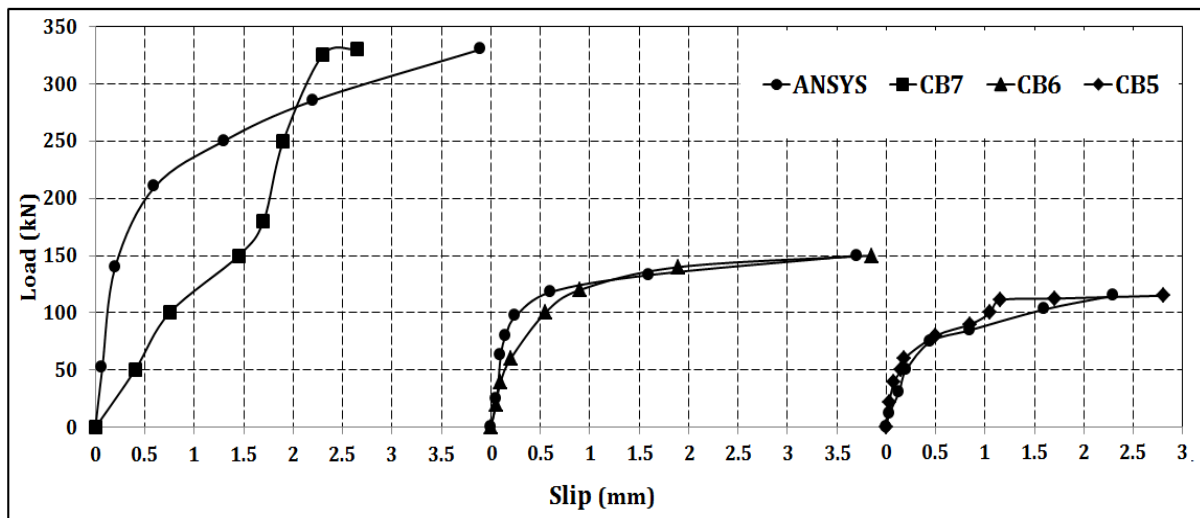


Figure (20): Slip-load curves from experimental test and finite element analysis (part 2).

سلوك وتحمل العتبات المركبة من الخرسانة المسلحة وانايبب الحديد ذات المقطع الدائري

وسام داود سلمان

مدرس، كلية الهندسة، جامعة ديالى

الخلاصة

يقدم هذا البحث دراسة تجريبية وتحليلية للتحري عن السلوك الانشائي للعتبات المركبة من الخرسانة المسلحة وانايبب الحديد ذات المقطع الدائري والمسندة اسنادا بسيطا تحت تأثير الحمل الخارجي والتي يرتبط العتب الخرسانى بالأنبوب المعدني الدائري بواسطة روابط قصرية. بالإضافة الى الخائص التقليدية للخرسانة وانايبب الحديد المكونة لهذا النوع من العتبات فان هذه العتبات تمتلك خصائص اخرى تفوقه وتفضله على باقي الانواع من العتبات مثال على ذلك سهولة تمرير الخدمات الميكانيكية للمنشآت والتي تسهل من عملية الانشاء ونقل الكلفة.

تضمن العمل اختبار سبع نماذج من العتبات المركبة من الخرسانة المسلحة وانايبب الحديد ذات المقطع الدائري وصولا الى حمل الفشل، حيث تم دراسة تأثير سمك وقطر الانبوب الحديدي على السلوك الانشائي للعتبات المركبة. أظهرت النتائج انه بزيادة سمك الانبوب الحديدي من (2 الى 6 ملم) فان تحمل العتبة المركبة وانحرافها الاقصى سيزداد بحدود (63.5%) و (75%) على التوالي. بينما اثبتت الدراسة عند زيادة قطر الانبوب الحديدي من (75 الى 200 ملم) فان التحمل الاقصى سيزداد بحدود (190.3%) والهطول الاقصى سيقبل بحدود (47%).

وبمقارنة النتائج التجريبية مع النتائج النظرية المستحصلة من التمثيل الرياضي للعتبات المركبة باستخدام التحليل العددي (طريقة العناصر المحددة باستخدام برنامج ANSYS) اظهرت النتائج بان هنالك تقارب كبير مع البيانات التجريبية.